

The Influence of Friction on Gait and Energy Efficiency of the Walking Robot Based on Rhythmic Control

H. Takemura, J. Ueda, Y. Matsumoto, T. Ogasawara

Nara Institute of Science and Technology, Takayama-cho, Ikoma, 630-0192, Nara, JAPAN

{hirosh-t,uedajun,yoshio,ogasawar}@is.aist-nara.ac.jp

Abstract

In this study, we focus on the slip that occurs during a walking motion. By using a 3-D dynamics simulation environment, we investigate the effects that of friction condition on the gait and the energy efficiency. A correlation is found between the energy efficiency and the stride in differing friction coefficients. The obtained results suggest that an effective walking can be attained by changing the walking pattern through the friction condition and the walking velocity.

1. Introduction

Neurophysiological studies of animals have revealed that the neural system contains a central pattern generator (CPG), which generates spatio-temporal patterns of activity for the control of rhythmic movements through the interaction of coupled neural oscillators [1]. Moreover, it has been reported that the centrally generated rhythm in the CPG is entrained by the rhythm of sensory signals at rates above and below the intrinsic frequency of the rhythmic activity [1]. Several simulation studies have focused on the dynamic interaction of neural oscillators with mechanical systems to understand the mechanisms that generates adaptive movements in insects [2], fish [3], and quadruped animals [4]. In the field of robotics, an increasing number of studies have implemented neural oscillators to control movements of real robots [5][6][7].

We have proposed a gait generation method that combines rhythm generators, reflexes, and sideways sways motion, which has achieved dynamic walking on regular and slop terrain [8]. However, the experiment has been conducted on one floor condition, and the influence of the slip has not been considered. Because the locomotion mechanism of the leg is often considered that the leg is stable on the supporting surface, several problems arise if a slip occurs on the supporting surface. In many of the conventional methods, when the robot loses its balance during its walk due to a slip, instead of sensing the slip itself, the problem is

dealt with by controlling the position and the dynamic condition of the entire robot. Therefore, unnecessary motion of the joints is generated. By detecting the slip and conducting appropriate compensative motions, unnecessary movements can be avoided, the energy efficiency is increased. As a result of such increase in energy efficiency, motion in environments with changing surface conditions can be made much easier. Considering the walking in an environment with varying frictions, it is also desirable to employ a gait appropriate to such variations. In this study, the effect of a gait on the energy efficiency in an environment with varying friction is investigated through a simulation. A correlation is presented between the energy efficiency and the walking cycle with different friction coefficients.

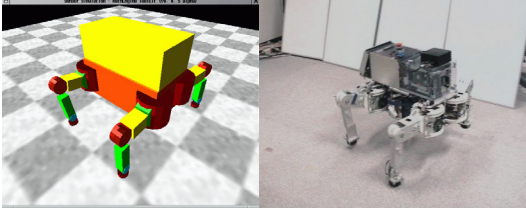
The organization of this paper is as follows. In section 2, the developed simulation environment is described in detail. In section 3, the CPG model and energy efficiency are defined. In section 4, the simulation experiment and its results are presented, and the effect of gait on energy efficiency is discussed. The paper ends with some conclusions and a suggestion for future works.

2. Dynamics Simulation Environment

2.1. MathEngine Toolkit

MathEngine Toolkit is adapted to build a simulation environment for our quadruped robot in the same manner as Kanehiro developed a simulator for a biped robot [9]. MathEngine plc. [10] has released software developing environments that allow real-time calculation of dynamics for computer games. MathEngine Toolkit is composed of the following three components; MathEngine Collision Toolkit (Mcd), MathEngine Dynamics Toolkit (Mdt) and MathEngine Simulation Toolkit (Mst).

Mcd is a toolkit which examines the interference between the objects. By omitting the examination of dis-



(a) A screen shot of the walking simulation (b) Quadruped robot

Figure 1: Developed simulation environment and real walking robot.

tant objects by collision culling and changing the layout of the memory, the processing speed has been accelerated. Mdt is a toolkit that simulates the dynamics of rigid objects. It has two integrator modes; one is the calculation of the free attachment objects and the other is the calculation of the combined rigid object trees that are constrained by collisions and joints. The Joints are simulated as springs with limited power generator. By using such a method, the instability that often occurs in simulation using a spring-damper model has been solved, and a relatively rough time step is enough compared to other simulator which requires very short sampling period. Mdt gives stable results even in relatively long time step such as ten milliseconds. Mst is a toolkit that mediates between Mdt and Mcd. Mst transfers the individual position and posture data from Mdt to Mcd, and the interference information from Mcd to Mdt.

2.2. Development of the simulation environment and evaluation of its performance

A simulation environment for a robot is developed by adding simulating functions for the sensors and the actuators to this Toolkit. Figure 1 (a) shows a screen shot of the walking simulation, and Figure 2 shows the software structure of the simulation environment. The software structure is designed so that the controller and the simulator can be performed separately. Therefore, the same controller can be used not only for the simulator but also for the real robot. The robot model is composed of links and joints. Each link is defined by a rigid object such as a box and a cylinder in Math-Engine toolkit. The data of the robot model is stored in the data file. By only changing the model data file, the simulation of various robots can be realized.

The simulation of the sensors is necessary to develop a control system that includes a sensory feedback. The current implementation provides angle sensors, angular velocity sensors, angular acceleration sensors, and force sensors. By using the developed simulator, the simulation of a walking robot with 16 degrees of free-

dom is calculable at a rate of approximately 12.23 [ms] for dynamical calculation and approximately 0.32[ms] for collision check (CPU: Pentium III 1GHz \times 2, OS: Linux). Even if the rendering process is included, the total calculation finishes within approximately twice of the time of the actual motion.

TITAN-VIII [11], a quadruped walking robot (Figure 1 (b)), is used for the experiments. Each leg has 3 degrees of freedom with a yaw axis which rotates around the primary joint and two roll axes which rotate around the second and the third joint respectively. Each joint is driven by a DC-motor, and the joint angle is detected by a potentiometer. Contact sensors are placed at the end of each leg, and a 3-axis gyro sensor and an inclinometer is attached to the body.

3. CPG Model and Network Model

3.1. Generation of a gait pattern

The neural oscillator model proposed by Matsuoka [12] and applied to the simulation of biped robots by Taga [13] is used. As show in Figure 3, a neural oscillator consist of two neurons (extensor neuron and flexor neuron) that are mutually inhibiting. It is represented by non-linear simultaneous differential equations given in Equation (1,2,3). Each leg of the robot is equipped with one of the neural oscillators.

$$\tau \dot{U}_{\{e,f\}i} = -U_{\{e,f\}i} + \sum_{j=1}^4 C_{ij} y_{\{e,f\}j} - AV_{\{e,f\}i} + u_i + F_{\{e,f\}i} \quad (1)$$

$$\tau \dot{V}_{\{e,f\}i} = -V_{\{e,f\}i} + y_{\{e,f\}i} \quad (2)$$

$$y_{\{e,f\}i} = \max(U_{\{e,f\}i}, 0) \quad (3)$$

The suffix e stands for the extensor neuron, f is the flexor neuron and i is for the i -th leg. U and V represent the internal state of the neurons. y is the output of the neuron, u is the drive input from the central neuron and F is the input from the sensor of the primary joint such as the joint angle. A is a fatigue parameter of the neuron, τ is the time parameter related to the walking cycle, C_{fe} is the coupling factor between the antagonistic neurons, C_{ij} is the coupling factor between the neuron's output of leg j and the neuron's input of leg i .

As can be seen in Equation (4), g_i , the output of the neural oscillator of leg i is calculated by the neuron's output of the extensors and flexors.

$$g_i = \alpha(U_{ei} - U_{fi}) \quad (4)$$

The outputs of the neural oscillators are directly trans-

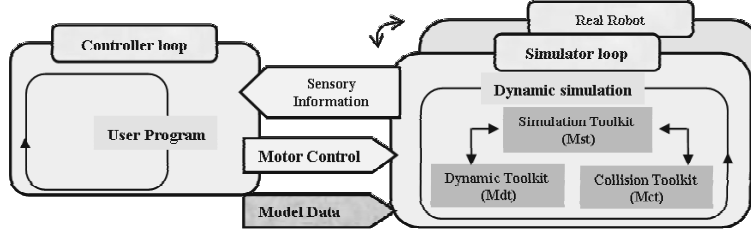


Figure 2: Software structure of the simulation environment.

mitted to the motors as the velocity reference of the primary joints ($\dot{\theta}_{pi}$). The swinging and supporting motion of the second joint θ_{si} and $\dot{\theta}_{si}$ are derived from the velocity of the primary joint as following Equation (5).

$$\begin{cases} \dot{\theta}_{si} = k \frac{d\dot{\theta}_{pi}}{dt} & (\dot{\theta}_{pi} \geq 0) : \text{swing motion} \\ \theta_{si} = 0 & (\dot{\theta}_{pi} < 0) : \text{support motion} \end{cases} \quad (5)$$

$k[\text{s/rad}]$

The third joint, which is not objectively used in this paper, is fixed as $\theta_{ti}=0$. By directly using the output of the neural oscillator, the trajectory of the leg's motion is determined. The trajectories are not directly planned as required in conventional model-based walking control methods. The neural oscillator network between the legs is shown in Figure 4. In this paper, the coupling factors between each leg are given by Equation (6), where only its sign is changeable and the magnitudes of the coupling factors are not considered.

$$C_{ij} = \begin{cases} +1 & : \text{Excitatory Connection} \\ 0 & : \text{No Connection} \\ -1 & : \text{Inhibitory Connection} \end{cases} \quad (6)$$

Various walking patterns can be generated changing only the combination of these values. Concretely, the phase difference of each leg can be controlled by determining C_{ij} as follows:

- walk gait : the phase difference of each leg is 90 degrees.
 $C_{12}=C_{21}=C_{13}=C_{24}=C_{34}=C_{43}=-1, C_{31}=C_{42}=+1$
- trot gait : the front and back leg, and the right and left leg are in opposite phase.
 $C_{12}=C_{21}=C_{13}=C_{31}=C_{24}=C_{42}=C_{34}=C_{43}=-1$
- pace gait : the front and back legs are in phase, and the right and left legs are in opposite phase.
 $C_{12}=C_{21}=C_{34}=C_{43}=-1, C_{13}=C_{31}=C_{24}=C_{42}=+1$
- bounce gait : the front and back leg are in opposite phase, and the right and left leg are in phase.
 $C_{12}=C_{21}=C_{34}=C_{43}=+1, C_{13}=C_{31}=C_{24}=C_{42}=-1$

3.2. Characteristics of the parameter

If the robot moves only on a horizontal plane, the velocity of the walking robot satisfies the following relationship:

$$V = \frac{S}{\beta T} \quad (7)$$

where S represents the stride of the leg in relation to the body, V is the walking velocity, T is the walking cycle, and β is the duty factor. In this paper, β is set to 0.5. To move at a certain velocity V , parameters (S, T) must be given, which means the parameter (τ, A, α) of the neural oscillators must be determined. The main purpose of the paper is to determine the combination of these parameters so that the best energy efficiency is obtained. If the fatigue constant A and the time constant τ are individually changed, the frequency and amplitude cannot be changed independently. By setting $\tau = A$ for simplicity, the relations between the parameters can be simplified so that S and T depend only on α and τ respectively.

3.3. Calculating the energy efficiency

In general, when the motor receives a stable energy supply, the torque decreases as the angular velocity increases, and the heat corresponding to the torque and the velocity is generated. The energy consumption e of each motor is given as follows:

$$e = \int \{ \delta(\Gamma(t)\omega(t)) + \gamma\Gamma^2(t) \} dt \quad (8)$$

$$\delta(x) = \begin{cases} 0 & (x \leq 0) \\ x & (x > 0) \end{cases} \quad (9)$$

where Γ is the torque, ω is the angular velocity and τ is a constant determined by the characteristic of the motor. The first term represents the outward mechanical power, and the second term represents the energy consumption through the heat loss. When the first term is negative, it means the energy from the outside is supplied and stocked in the motor, but motors usually

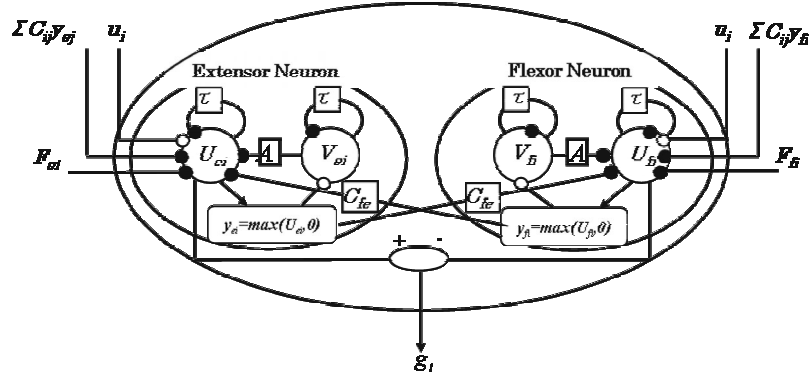


Figure 3: Neural oscillator as a model of the CPG.

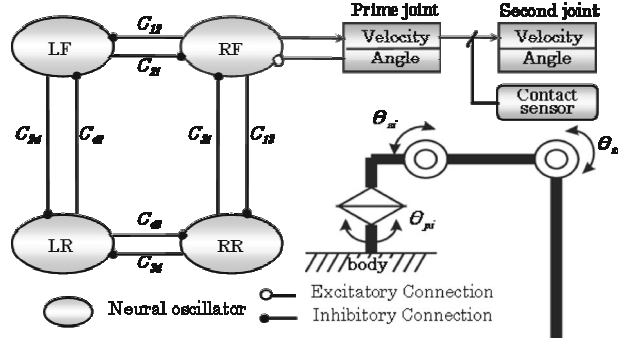


Figure 4: Neural oscillator network model.

cannot store such energy, therefore, in this paper, the mechanical power is set to zero when the first term is negative. The following specific power is used as the definition of the energy efficiency to determine the optimal walking parameters:

$$\epsilon = \frac{E}{VT} = \frac{\beta}{S} E \quad (10)$$

where E is the sum of the energy consumed by each motor while the robot walks a distance of VT . This equation gives the amount of energy consumed when the walking robot is moving a unit migration distance. Thus a smaller value of ϵ represents higher energy efficiency.

4. Simulation and Results

In this section, the effects of the friction condition on the gait and the energy efficiency will be examined by a walking simulation in the environment with varying friction coefficients. A 3-D dynamics simulation environment described in the section 2 is used for the simulation environment, and the values of a real robot TITAN-VIII [11] (Figure 1(b)) used for the robot model. For the surface condition, a flat plane and the

friction coefficients ($\mu=0.4, 0.6, 1.0$) that the general conditions of slippery, normal and sticky are chosen. The method of gait generation is as shown in the section 3.1. A constant value $\beta=0.5$ is used for the duty factor. The simulations of walking under each friction condition have been conducted with α being changed by 0.005 in $[0.02 \leq \alpha \leq 0.05]$ and τ being changed by 0.05 in $[0.2 \leq \tau \leq 0.5]$ respectively. The relation between α, τ and V , and the relation between α, τ and ϵ are calculated. Each simulation is started from a standing-still followed by 20 seconds of walking. The walking velocity and the energy efficiency are calculated for 10 to 20 seconds of steady-state.

Figure 5 shows the relation between the walking velocity and the energy efficiency due to the varying friction coefficients. The relation between the walking velocity and the energy efficiency is such that the energy efficiency is low at a low speed regardless of the friction coefficient. As the walking velocity increases, the energy efficiency increases (Figure 5). These results match well to those of a bioengineering research conducted on horses [1].

The effect of friction can be seen that the energy efficiency tends to decline at a low velocity, a friction coefficient of $\mu=0.6$ is most efficient after the velocity

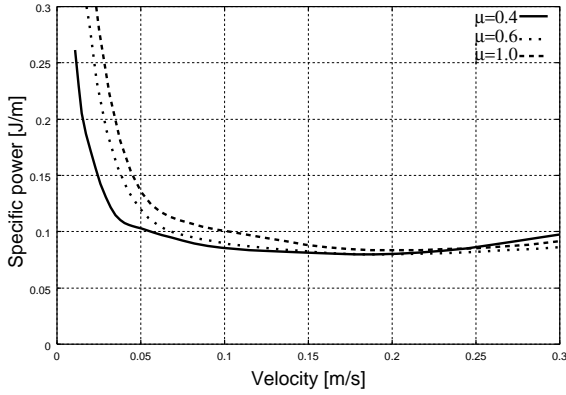


Figure 5: The relation between the velocity and specific power.

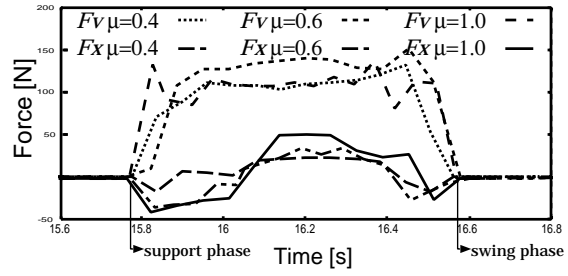
exceeded $V=0.2$.

In general, the energy efficiency increases when the friction increases. However the results of this experiment showed the opposite. Hereafter, the causes of such results are discussed, and a relation between specific resistance and the stride/walking cycle of varying friction coefficients are considered.

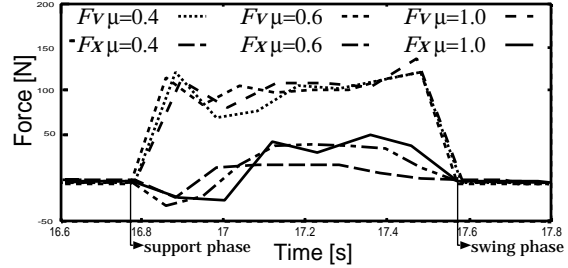
5. Discussion

In general, it is thought that a slip occurs and the driving force is small when the friction level is small, while a larger friction provides the supporting leg a larger driving force. This trait can be seen strongly at the beginning of a walk. The average time from the beginning to the time when the walk reaches a steady-state becomes shorter as the friction increases. In other words, when the friction is small, a prominent slip occurs at the beginning of the walk. Therefore time is required until a steady condition is attained because the driving force can not be gained. In our experiment, the energy efficiency is calculated under steady-state, and this influence is not considered.

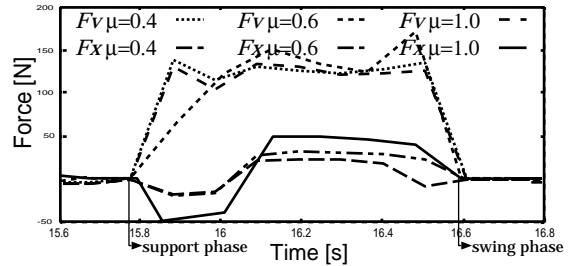
During the steady-state, the floor reaction force works in the opposite of the walking direction of the driving force when the leg contacts the supporting surface, because inertia force works on the robot's body. In some cases, such reaction force may act as a brake under the influence of the timing of contact of the swing leg. The reaction forces of varying frictions and walking velocities $V=0.1, 0.2, 0.3$ ($\alpha=0.02, 0.035, 0.045$ are used for the walking stride, namely the trajectory of the leg is fixed and only the walking cycle is changed) are shown in Figure 6. F_v is the vertical direction force, F_x is the movement direction force. In each condition, F_x works in the opposite direction of



(a) Velocity 0.1 [m/s], Walking stride $\alpha=0.02$



(b) Velocity 0.2 [m/s], Walking stride $\alpha=0.035$



(c) Velocity 0.3 [m/s], Walking stride $\alpha=0.045$

Figure 6: The reaction at half walking cycle.

driving when the leg contacts the supporting surface, and acts as a brake. This force increases as the friction increases. It can also be seen that the leg is dragged when changing from support motion to swing motion in $V=0.1$. However, the leg is not dragged and smooth changes are performed in $V=0.2$. When the velocity exceeded $V=0.2$, a friction coefficient of $\mu=0.4$ shows a decline in the energy efficiency (Figure 5). When the friction is small, the inertia force becomes weakly as a brake, while the driving force of the kick becomes difficult to gain at the same time. In addition, from this relation between the brake effect and the driving force, to increase the velocity beyond a certain amount more energy is needed, resulting in a decrease of efficiency. Because this experiment uses a quadruped walking robot, a loss of balance caused by a slip that resulted in a fall of the robot as seen in biped robots did not occur.

The relation between the friction and the optimal walking cycle τ is shown in Table 1. From this Table,

Table 1: The relation between the friction and the optimal walking cycle.

		Friction Coefficient		
		$\mu=0.4$	$\mu=0.6$	$\mu=1.0$
Velocity	$V=0.1$ [m/s] $\alpha=0.02$	$\tau=0.20$	$\tau=0.35$	$\tau=0.25$
	$V=0.2$ [m/s] $\alpha=0.035$	$\tau=0.30$	$\tau=0.30$	$\tau=0.30$
	$V=0.3$ [m/s] $\alpha=0.045$	$\tau=0.25$	$\tau=0.40$	$\tau=0.30$

it can be seen that τ becomes smaller when the friction coefficient is $\mu=0.4$ and the walking velocity is $V=0.1$. A smaller value of τ represents a faster walking cycle which leads to an effective walk as stated in the previous paragraph. In the case of $V=0.2$, the value of τ is the same for all the friction coefficients, and this is reflected in the energy efficiency which is almost the same (Figure 5). When the velocity value of $V=0.3$ and the friction value of $\mu=0.6$, it can be see that a large value of τ ; at the same time this is the case where the energy consumption is lower (Figure 5). Therefore, when the friction is small and the speed is low, a walking with a small stride and a fast cycle results in a better energy efficiency. When the friction is large and the speed is high, a walk with a wide stride at a slow walking cycle is effective. Namely, in an environment with varying frictions, there is a difference in the form of the effective gait.

6. Conclusions and Future Works

In this study, we focused on the slip which occurs during the walking motion. By using a 3-D dynamics simulation environment, we examined the effect that the friction condition has on the gait and the energy efficiency, namely:

- The energy efficiency increases as the velocity increases regardless the friction condition.
- When the walking velocity is low, the energy efficiency increases as the friction decreases. When the walking velocity increases, the middle friction condition is the most efficient.
- There is a difference in the form of the effective gait in an environment with varying frictions.

The obtained results suggest that an effective walking can be attained by changing the walking pattern in accordance with the friction condition and the walking velocity. The change of the friction can hypothetically be replaced by the walking on a slope, thus we think that this study may discover an appropriate walking

pattern on a slope. Future work includes introducing a slip reflex in which the CPG is entrained by the information of the “slip of the leg”, and developing a gait generating algorithm that is adaptable to the environment with varying friction conditions. Furthermore, the duty factor has been fixed and only the change in gait has been taken into consideration in this paper. However, one of the characteristics of the walking motion of living creatures is the variation of the duty factor in accordance to the walking velocity. Further study must be conducted on the energy efficiency in relation to the change in duty factor, as well as on the stability of the posture during the walking motion.

References

- [1] Gillner, S., 1985, “Neurobiological Bases of rhythmic motor acts in vertebrate”, *Science*, Vol. 228, pp.143-149.
- [2] Kimura, S., Yano, M., Shimizu, H., 1993, “A selforganizing model of walking patterns of insects”, *Biological Cybernetics*, Vol. 69, 183-193.
- [3] Ekeberg, O., 1993, “A combined neuronal and mechanical model of fish swimming”, *Biological Cybernetics*, Vol.69, 363-374.
- [4] Wadden, T., Ekeberg, O., 1998, “A neuro-mechanical model of legged locomotion: single leg control”, *Biological Cybernetics*, Vol. 79, 161-173.
- [5] Miyakoshi, S., Yamakita, M., Furata, K., 1994, “Juggling control using neural oscillators”, *Proc. IEEE/RSJ IROS94*, 2, 1186-1193.
- [6] Kimura, H., Sakurama, K., Akiyama, S., 1998, “Dynamic walking and running of the quadruped using neural oscillators”, *Proc. IEEE/RSJ, IROS98*, 1, 50-57.
- [7] Williamson, M., M., 1998, “Neural control of rhythmic arm movements”, *Neural Networks*, 11, 1379-1394.
- [8] Takemura, H., Matsumoto, Y., Ogasawara, T., 2001, “Dynamic walking of an autonomous quadruped robot based on rhythm generation”, *Proc. CLAWAR2001*, pp.727-734.
- [9] Kanehiro, F., 2001, “Virtual robot body driven by fast dynamics simulation toolkit for game development”, *Proc. ROBOMECON1*, paper number 2P2-H3. (in Japanese)
- [10] <http://www.mathengine.com>, MathEngine plc.
- [11] Hirose, S. and Arikawa K., 1996, “Development of quadruped walking robot TITAN-VIII”, *Proc. IEEE/RSJ IROS96*, pp.208- 214.
- [12] Matsuoka, K., 1985, “Sustained oscillations generated by logical cybernetics”, *Biological Cybernetics*, Vol. 52, pp.367-376.
- [13] Taga, G., 1995, “A model of the Neuro-Musculo-Skeletal system for human locomotion”, *Biological Cybernetics*, Vol. 73, pp.97-111.